Vol 16 No 10, October 2007
1009-1963/2007/16(10)/2938-08
Chinese Physics
© 2007 Chin. Phys. Soc.
and IOP Publishing Ltd

Generalized oscillator strengths for some higher valence-shell excitations of krypton atom*

Zhu Lin-Fan(朱林繁)†, Zhang Fang-Xin(张放心), Cheng Hua-Dong(成华东), Yuan Hui(袁 慧), Yuan Zhen-Sheng(苑震生), Li Wen-Bin(李文斌), Liu Xiao-Jing(刘小井), and Xu Ke-Zun(徐克尊)

Hefei National Laboratory for Physical Sciences at Microscale, Department of Modern Physics, University of Science and Technology of China, Hefei 230026, China

(Received 8 November 2006; revised manuscript received 1 April 2007)

The valence-shell excitations of krypton atom have been investigated by fast electron impact with an angle-resolved electron-energy-loss spectrometer. The generalized oscillator strengths for some higher mixed valence-shell excitations in 4d, 4f, 5p, 5d, 6s, 6p, 7s ← 4p of krypton atom have been determined. Their profiles are discussed, and the generalized oscillator strengths for the electric monopole and quadrupole excitations in 5p ← 4p are compared with the calculations of Amusia *et al.* (*Phys. Rev.* A **67** 022703 (2003)). The differences between the experimental results and theoretical calculations show that more studies are needed.

Keywords: generalized oscillator strength, electric multipolarity, krypton
PACC: 3270C, 3480, 3480D

1. Introduction

The generalized oscillator strengths (GOSs), differential cross sections (DCSs), integrated cross sections and total cross sections can be determined by electron-impact excitation, and these cross sections have wide applications in a variety of fields, such as plasma physics, astrophysics, etc.[1−5] For a krypton atom, its cross sections are very useful in the plasma diagnostics for the thermonuclear reactor, plasma processing of flat-panel displays technology, and pumping mechanisms in KrF gas–laser systems. As a heavy rare gas, the excited energy level structure of krypton atom is well described by the intermediate coupling, while its ground state is a closed-shell $^1S_0$ state of LS coupling, which makes krypton a typical system to study the valence-shell excitation mechanism and dynamics relating to two different coupling schemes.[6,7] However, there are tremendous challenges to theoretical models because of the complications of many-electron heavy atom and non-LS-coupling nature in krypton. Furthermore, a comparison of the shapes as well as the absolute magnitudes of the measured and calculated GOSs and DCSs can help to evaluate computational procedures, determine correct spectral assignments, as well as test the accuracy of the wavefunction.[2,8−14]

When the incident electron is sufficiently fast, the influence of the incident electron on an atom or molecule can be regarded as a sudden and small external perturbation, and the exchange effect is negligibly small.[1] Therefore, the cross section can be factorized into two factors: one is to deal with the incident particle only and the other is to treat the target only. The GOS is defined as[1,15,16] (in atomic units (a.u.))

$$f(E,K) = \frac{E}{2}\frac{p_0}{p_\mathrm{a}}K^2\frac{\mathrm{d}\sigma}{\mathrm{d}\Omega} = \frac{2E}{K^2}|<\Psi_n|\sum_{j=1}^{N}\exp(\mathrm{i}\boldsymbol{K}\cdot\boldsymbol{r}_j)|\Psi_0>|^2, \quad (1)$$

where E and K are the excitation energy and momentum transfer, while p_0 and p_a are the incident and scattered electron momenta, respectively. $f(E,K)$ and $\mathrm{d}\sigma/\mathrm{d}\Omega$ denote GOS and DCS while Ψ_0 and Ψ_n are N electrons wave functions for initial and final states, respectively. $\boldsymbol{r}_j$ is the position vector of the jth electron.

The previous experimental and theoretical studies of the DCS and GOS of krypton atom have been summarized in our recent paper,[17] therein the GOSs and DCSs for the lower excitations of 5s, 5p ← 4p are investigated. The present work is an addition to our previous measurements.[17] It should be emphasized that besides our recent studies most of the previous

*Project supported by the National Natural Science Foundation of China (Grant No 10474089).
†E-mail: lfzhu@ustc.edu.cn

works concentrated on DCSs investigations of the excitations to 5s and 5s′ (See Ref.[17] and the references therein). The only experimental GOSs for some excitations to 5p and 4d were reported in Refs.[6,17,18], and the multipolarities for these transitions were also elucidated clearly.[6] Theoretically, Amusia *et al*[19] calculated the GOSs for the monopole and quadrupole excitations of $(n+1)\mathrm{p}, (n+2)\mathrm{p} \leftarrow n\mathrm{p}$ of noble atoms from neon to xenon, and they pointed out that there were no high-resolution experimental data for comparison. Herein the main purposes of this high-resolution work are to provide the new experimental GOSs for some higher mixed transitions of 4d, 4f, 5p, 5d, 6s, 6p, $7\mathrm{s} \leftarrow 4\mathrm{p}$ and to test the theoretical calculations.[19]

2. Experimental and theoretical methods

2.1. Experimental method

The angle-resolved electron-energy-loss spectrometer (AREELS) used in this experiment has been described in detail in Refs.[20–22]. Briefly, it consists of an electron gun, a hemispherical electrostatic monochromator made of aluminium, a rotatable energy analyser of the same type, an interaction chamber, a number of cylindrical electrostatic lenses, and a one-dimensional position sensitive detector to detect the scattered electrons. All of these components are enclosed in four separate vacuum chambers made of stainless steel. The impact energy of the spectrometer can be varied from 1 to 5 keV. For the present measurement the impact energy was set at 2500 eV and the energy resolution was 65 meV [full width at half maximum (FWHM)]. The background pressure in the vacuum chamber was 5×10^{-5} Pa. The scattering angle was calibrated by the angular distribution of the $4\mathrm{p}^5(5\mathrm{s}+5\mathrm{s}') \leftarrow 4\mathrm{p}^6$ inelastic scattering signals around the geometry nominal 0°. The angular resolution was about 1.2° FWHM at present.

In this work, the electron-energy-loss spectra in the energy region of $9-15$ eV were measured from scattering angles 1.0° to 8.5° with an interval of 0.5°. A typical electron energy loss spectrum is shown in Fig.1. The assignments for the peaks from A to I can be found in our recent work (see Table 1 in Ref.[6]), while the assignments for peaks J, K, and L are shown in Table 1. It can be noticed that each of peaks G, H, and I includes two heavily overlapped excitations (see Table 1 in Ref.[6]), while Table 1 shows that each of peaks J, K, and L includes heavily overlapped transitions. Therefore, in the least square fitting procedure, we assumed that all excitations had the same peak profile which was determined by fitting the first two excitations of $4\mathrm{p}^5 5\mathrm{s}[3/2]_1$ (peak A) and $4\mathrm{p}^5 5\mathrm{s}'[1/2]_1$ (peak B). Then the intensities of all excitations (their energy positions were taken from Moore[23]) were obtained. However, only experimental GOSs for peaks G, H, I, J, K, and L were given since their intervals were near or larger than the experimental energy resolution. Furthermore, by combining the calculated intermediate coupling coefficients with the experimental GOSs,[6,17] the separated GOSs for the excitations included in peaks G and H were determined (the method is discussed in detail in our recent work[6]).

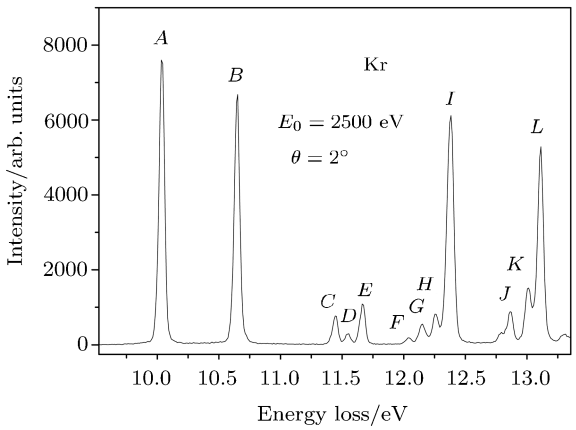


Fig.1. A typical electron-energy-loss spectrum of krypton atom.

It is well known that the double scattering processes can result in large experimental errors in the GOS and DCS measurements as shown by the results of Ref.[21]. Because the intensity of double scattering process is proportional to the square of pressure, while the intensity of the single scattering process is proportional to pressure, the relationship between the measured intensity ratio and pressure is expressed as[17]

$$\frac{I_{\mathrm{p}}(\theta)}{I_{\mathrm{ref}}(\theta)} \approx \left(\frac{I_{\mathrm{p}}(\theta)}{I_{\mathrm{ref}}(\theta)}\right)_{P=0} + c(\theta)P. \qquad (2)$$

Here $c(\theta)$ is a coefficient which depends on the scattering angle and the cross section of the measured excitation. $I_{\mathrm{p}}(\theta)$ and $I_{\mathrm{ref}}(\theta)$ represent the intensity of the excitation to be studied and that of the dipole forbidden excitations of C+D+E, respectively. The value of $(I_{\mathrm{p}}(\theta)/I_{\mathrm{ref}}(\theta))_{P=0}$, which is proportional to the ratio of the cross sections, was obtained for each scattering angle by linear least-square fitting. As an example,

some results for double scattering correction of the peak I are shown in Fig.2, and the lines represent the results for the least-square fitting to the data points. In addition, the finite angular resolution has great influence on the GOSs measured at small angles. The influence of angular resolution was corrected by modifying the momentum transfer square K^2 in Eq.(1) to average momentum transfer $\langle K^2\rangle$[24] as follows:

$$f(E,K) = \frac{E}{2}\frac{p_0}{p_a}\langle K^2\rangle\frac{d\sigma}{d\Omega} = \frac{E}{2}\frac{p_0}{p_a}(p_0^2+p_a^2-2p_0p_a e^{-\alpha^2/2}\cos\theta_0)\frac{d\sigma}{d\Omega}, \quad (3)$$

where $\alpha = \Delta\theta/\sqrt{8ln2}$, θ_0 and $\Delta\theta$ refer to the measured angle and the angular resolution (FWHM), respectively.

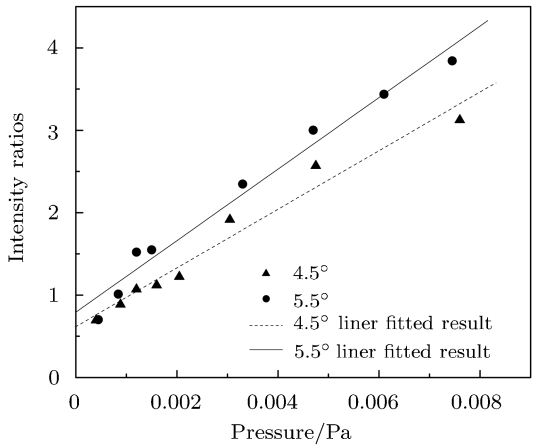


Fig.2. Intensity ratios $I_p(\theta)/I_{ref}(\theta)$ as a function of pressure for peak I.

Then, using the absolute GOSs for the dipole forbidden excitations of $C + D + E$ determined in our recent work[17] and the obtained ratio $(I_p(\theta)/I_{ref}(\theta))_{P=0}$, the absolute GOSs for the peaks of F, G, H, I, J, K and L were determined (the data are shown in Table 2).

It can be seen from Eq.(1) that the errors of GOSs mainly come from the differential cross section δ_{DCS}, the momentum transfer δ_{K^2} and the normalizing procedure δ_n. Among them, the errors of DCSs come from the statistics of counts δ_s, the deconvolution procedure δ_d, as well as the pressure correction δ_p. The errors of K^2 come from the angle determination δ_r and the angular resolution $\delta_{r'}$. In this work, the range of each error is $\delta_{DCS} = 5\% - 12\%$ ($\delta_s \le 5\%$, $\delta_d \le 10\%$, $\delta_p \le 5\%$), $\delta_{K^2} = 1\% - 8\%$ ($\delta_r \le 5\%$, $\delta_{r'} \le 5\%$), and $\delta_n \le 10\%$, respectively. The total errors are less than 18% and shown in the corresponding figures.

2.2. Calculational method

The calculations of the intermediate coupling coefficients for the presently concerned levels of Kr were performed with the Cowan code.[25] The method of calculation was described in detail by Clark *et al*,[26,27] and summarized in our recent work.[28]

For the present calculations, a 21 configuration basis set was used, and the calculated excitation energies are consistent with the Moore levels[23] within 0.17 eV. The calculated intermediate coupling coefficients and the energy levels that are involved in the peaks F, G, H, I, J, K and L are listed in Table 1. The other calculated intermediate coupling coefficients and the energy levels that are involved in the peaks A, B, C, D, and E have been listed in our previous work.[6]

3. Results and discussion

In Table 1 we just present the significant intermediate coupling coefficients ($\ge$ 0.1) and the transition multipolarity for the peaks from F to L. According to the calculated intermediate coefficients and the method to determine the transition multipolarities,[6] the observed transitions (peaks $F - L$) in the energy region of 11.8–13.2 eV shown in Fig.1 consist of the electric monopole transitions of $4p^5 5p'[1/2]_0$ and $4p^5 6p[1/2]_0$, the electric dipole transitions of $4p^5 4d[1/2]_1$, $4p^5 4d[3/2]_1$, $4p^5 6s[3/2]_1$, $4p^5 5d[1/2]_1$, $4p^5 4d'[3/2]_1$, $4p^5 6s[1/2]_1$, $4p^5 5d[3/2]_1$ and $4p^5 7s[3/2]_1$, the electric quadrupole transitions of $4p^5 5p'[3/2]_2$, $4p^5 6p[5/2]_2$, $4p^5 6p[3/2]_2$, $4p^5 4f[3/2]_2$ and $4p^5 4f[5/2]_2$, the electric octupole transitions of $4p^5 4d[7/2]_3$, $4p^5 4d[5/2]_3$, $4p^5 4d'[5/2]_3$, $4p^5 5d[7/2]_3$ and $4p^5 5d[5/2]_3$, as well as the electric hexadecapole transition of $4p^5 4f[7/2]_4$. The GOSs for these transitions are listed in Table 2, herein the method to determine the individual GOSs in peaks G and H was described in our previous work.[6]

The GOSs for the electric dipole allowed transitions of peak F and I are shown in Figs.3 and 4, respectively. Since the spin-forbidden transition is negligible small for fast electron impact[1] and the initial ground state of Kr is singlet, the GOSs of these excitations are only determined by their singlet component.[6] It is also noticed that the intermediate coupling coefficient of the only existed singlet $4p^5 4d\ ^1P_1$ in peak F is about one-sixth of that of the same singlet in peak I (see Table 1 in Ref.[6]),

and moreover, peak I includes the contributions from other transitions, thus the phenomenon that the GOS of peak F is much lower than that of peak I can be easily understood. So the GOS of peak F is only presented for K^2 up to 0.7 a.u. because of the statistical error beyond this region being very large. From Fig.3 it can be seen that the GOS curve decreases with the increasing of the momentum transfer at lower values of K^2, which is the typical character of the dipole-allowed transition. Based on the Lassettre's limit theorem,[29] the GOS converges to the optical oscillator strength (OOS) as $K^2 \to 0$. The behaviour of the GOS near $K^2 = 0$ is illustrated as

$$f(E_0, K) = \frac{1}{(1+x)^6}\Big[f_0 + \sum_{n=1}^{m} f_k \Big(\frac{x}{1+x}\Big)^n\Big], \quad (4)$$

where f_0 is the OOS and

$$x = K^2/\alpha^2$$

with

$$\alpha = (2I)^{1/2} + [2(I-E)]^{1/2}$$

with I and E being the ionization threshold and excitation energy, respectively. The solid line in Fig.3 represents the fitted result with Eq.(4). The extrapolated OOS is 0.0054, which is in good agreement with the value of 0.0052 determined by dipole (e, e) method.[30] Furthermore, the GOS for the electric dipole transition of $4p^5 4d\ ^1P_1 \leftarrow 4p^6\ ^1S_0$ can be obtained through dividing the GOS for peak F by the square of the corresponding intermediate coupling coefficient.[6]

Table 1. The assignments for the peaks from J to L. The energy values are taken from Moore.[23] E_0, E_1, E_2, E_3, and E_4 represent electric monopole, electric dipole, electric quadrupole, electric octupole, and electric hexadecapole excitations from the ground state ($4p^6\ ^1S_0$), respectively.

Peak	J L designation	Intermediate coupling	Transition	Energy/eV Cowan	Energy/eV Moore
Ground state	$4p^6$	$0.9973(4p^6\ ^1S_0)$		0	0
F	$4p^5 4d[1/2]_1$	$0.9411(4p^5 4d\ ^3P_1)+0.1029\ (4p^5 4d\ ^1P_1)$ $+0.2471(4p^5 4d\ ^3D_1) - 0.1185(4p^5 5s\ ^3P_1)$ $+0.1088(4p^5 5d\ ^3P_1)$	E_1	12.059	12.037
G	$4p\ ^5 5p'[3/2]_2$	$0.6618(4p\ ^5 5p\ ^3D_2) - 0.4709(4p^5 5p\ ^3P_2)$ $+0.5817(4p^5 5p\ ^1D_2)$	E_2	12.106	12.144
	$4p^5 4d[7/2]_3$	$0.7837(4p^5 4d\ ^3F_3)+0.1861(4p^5 4d\ ^3D_3)$ $-0.5906(4p^5 4d\ ^1F_3)$	E_3	12.177	12.179
H	$4p^5 5p'[1/2]_0$	$0.7261(4p^5 5p\ ^3P_0)+0.6601(4p^5 5p\ ^1S_0)$ $-0.1687(4p^5 6p\ ^1S_0)$	E_0	12.234	12.257
	$4p^5 4d[5/2]_3$	$0.2226(4p^5 4d\ ^3F_3)+0.8031(4p^5 4d\ ^3D_3)$ $+0.5494(4p^5 4d\ ^1F_3)$	E_3	12.294	12.284
I	$4p^5 4d[3/2]_1$	$0.6338(4p^5 4d\ ^3D_1) - 0.6057(4p^5 4d\ ^1P_1)$ $+0.2037(\ 4p^5 5d\ ^1P_1)+0.3250(4p^5 6s\ ^1P_1)$ $-0.2402(4p^5 6s\ ^3P_1)$	E_1	12.403	12.354
	$4p^5 6s[3/2]_1$	$0.2863(4p^5 4d\ ^1P_1)+0.1220(4p^5 4d\ ^3P_1)$ $-0.2495(4p^5 4d\ ^3D_1) - 0.5437(4p^5 6s\ ^3P_1)$ $+0.7278(4p^5 6s\ ^1P_1)$	E_1	12.428	12.385
J	$4p^5 6p[5/2]_2$	$0.69682(4p^5 6p\ ^3D_2) - 0.17637(4p^5 6p\ ^3P_2)$ $+0.68835(\ 4p^5 6p\ ^1D_2)$	E_2	12.777	12.785
	$4p^5 6p[3/2]_2$	$-0.19752(4p^5 6p\ ^3D_2)+0.88355(4p^5 6p\ ^3P_2)$ $+0.41975(4p^5 6p\ ^1D_2)$	E_2	12.803	12.815
	$4p^5 4d'[5/2]_3$	$+0.57168(4p^5 4d\ ^3F_3)+0.56118(4p^5 4d\ ^3D_3)$ $+0.58804(4p^5 4d\ ^1F_3)+0.10256(4p^5 5d\ ^3F_3)$	E_3	12.802	12.857
	$4p^5 6p[1/2]_0$	$-0.63153(4p^5 6p\ ^3P_0) - 0.25868(4p^5 7p\ ^3P_0)$ $+0.69429(4p^5 6p\ ^1S_0)+0.20418(4p^5 8p\ ^3P_0)$	E_0	12.877	12.865
	$4p^5 5d[1/2]_1$	$-0.39328(4p^5 5d\ ^3D_1)+0.25223(4p^5 6s\ ^3P_1)$ $-0.52421(4p^5 5d\ ^3P_1)+0.10606(4p^5 6d\ ^3P_1)$ $-0.30239(4p^5 6d\ ^3P_1) - 0.2683(4p^5 7d\ ^3P_1)$ $-0.27347(4p^5 9s\ ^3P_1)+0.25301(4p^5 8d\ ^3P_1)$ $+0.27976(4p^5 8d\ ^3D_1)+0.24867(4p^5 5d\ ^1P_1)$	E_1	12.983	12.870

Table 1. continued

K	$4p^5 4d'[3/2]_1$	$-0.34512(4p^5 6s\ ^1P_1)$-$0.52963(4p^5 4d\ ^3D_1)$ $+0.47593(4p^5 4d\ ^1P_1)+0.34906(4p^5 5d\ ^3P_1)$ $-0.30277(4p^5 5d\ ^3D_1)+0.14764(4p^5 6d\ ^3P_1)$ $+0.21275(4p^5 5d\ ^1P_1)+0.15148(\ 4p^5 6d\ ^1P_1)$ $+0.11143(4p^5 7d\ ^1P_1)+0.20377(4p^5 8d\ ^1P_1)$	E_1	12.869	13.004
	$4p^5 5d[7/2]_3$	$-0.16399(4p^5 4d\ ^1F_3)+0.72622(4p^5 5d\ ^3F_3)$ $-0.20795(4p^5 5d\ ^3D_3)+0.11361(4p^5 7d\ ^3F_3)$ $-0.60192(4p^5 5d\ ^1F_3) - 0.12162(4p^5 8d\ ^3F_3)$	E_3	12.999	13.008
	$4p^5 6s[1/2]_1$	$0.65756(4p^5 6s\ ^1P_1) - 0.44917(4p^5 4d\ ^3D_1)$ $-0.15628(4p^5 4d\ ^1P_1) - 0.28411(4p^5 5d\ ^3D_1)$ $-0.50153(4p^5 6s\ ^3P_1)$	E_1	13.018	13.036
	$4p^5 5d[5/2]_3$	$0.12380(4p^5 4d\ ^1F_3) - 0.16690(4p^5 5d\ ^3F_3)$ $+0.83806(4p^5 5d\ ^3D_3)+0.47660(4p^5 5d\ ^1F_3)$	E_3	13.035	13.044
L	$4p^5 5d[3/2]_1$	$0.10368(4p^5 4d\ ^3P_1)+0.54373(4p^5 4d\ ^1P_1)$ $+0.55676(4p^5 5d\ ^3D_1) - 0.43851(4p^5 6s\ ^3P_1)$ $-0.26631(4p^5 5d\ ^3P_1) - 0.13162(4p^5 6d\ ^3P_1)$ $-0.12240(4p^5 7d\ ^1P_1) - 0.13436(4p^5 9s\ ^1P_1)$ $+0.15415(4p^5 8d\ ^3D_1)+0.15873(4p^5 5d\ ^1P_1)$	E_1	13.165	13.099
	$4p^5 7s[3/2]_1$	$0.58062(4p^5 7s\ ^3P_1)+0.80093(4p^5 7s\ ^1P_1)$	E_1	13.112	13.114
	$4p^5 4f[3/2]_2$	$0.73866(4p^5 4f\ ^3D_2)+0.67339(4p^5 4f\ ^1D_2)$	E_2	13.127	13.138
	$4p^5 4f[5/2]_2$	$0.78301(4p^5 4f\ ^3F_2) - 0.41034(4p^5 4f\ ^3D_2)$ $+0.46668(4p^5 4f\ ^1D_2)$	E_2	13.134	13.145
	$4p^5 4f[7/2]_4$	$0.86271(4p^5 4f\ ^3F_4)+0.50555(4p^5 4f\ ^1G_4)$	E_4	13.137	13.148

Table 2. The GOSs for peaks F, G, H, I, J, K and L. Square brackets denote the power of ten.

K^2/a.u.	F	G		H		I	J	K	L
		$4p^5 5p'[3/2]_2$	$4p^5 4d[7/2]_3$	$4p^5 5p'[1/2]_0$	$4p^5 4d[5/2]_3$				
0.07	4.46[–3]	4.58[–3]		6.50[–3]		2.08[–1]	2.02[–2]	4.07[–2]	1.46[–1]
0.14	3.17[–3]	7.39[–3]	4.70[–4]	9.51[–3]	4.10[–4]	1.32[–1]	1.92[–2]	3.23[–2]	9.67[–2]
0.24	1.77[–3]	6.46[–3]	2.02[–3]	9.07[–3]	1.77[–3]	1.04[–1]	1.70[–2]	2.46[–2]	7.51[–2]
0.36	1.11[–3]	5.53[–3]	1.60[–3]	6.99[–3]	1.39[–3]	5.05[–2]	1.18[–2]	1.24[–2]	3.89[–2]
0.52	5.54[–4]	3.66[–3]	4.03[–3]	4.54[–3]	3.52[–3]	2.49[–2]	7.93[–3]	8.22[–3]	2.05[–2]
0.70	3.58[–4]	2.36[–3]	5.58[–3]	2.97[–3]	4.87[–3]	1.15[–2]	8.21[–3]	7.97[–3]	1.00[–2]
0.90		1.31[–3]	5.35[–3]	1.67[–3]	4.67[–3]	6.01[–3]	6.25[–3]	5.83[–3]	5.76[–3]
1.15		4.35[–4]	4.20[–3]	1.14[–3]	3.66[–3]	1.87[–3]	4.28[–3]	5.07[–3]	2.03[–3]
1.41		2.01[–4]	3.73[–3]	8.69[–4]	3.26[–3]	1.51[–3]	3.68[–3]	4.60[–3]	1.31[–3]
1.70		1.63[–4]	2.92[–3]	7.14[–4]	2.55[–3]	1.43[–3]	2.62[–3]	3.59[–3]	9.97[–4]
2.02		3.14[–4]	2.84[–3]	7.44[–4]	2.48[–3]	1.89[–3]	2.97[–3]	3.73[–3]	1.29[–3]
2.37		4.82[–4]	2.42[–3]	5.85[–4]	2.11[–3]	1.84[–3]	2.43[–3]	3.02[–3]	1.88[–3]
2.75		6.26[–4]	1.86[–3]	1.16[–3]	1.62[–3]	1.87[–3]	2.51[–3]	2.61[–3]	2.13[–3]
3.15		7.03[–4]	1.60[–3]	1.30[–3]	1.40[–3]	2.21[–3]	2.71[–3]	3.92[–3]	4.32[–3]
3.59		7.51[–4]	8.47[–4]	2.03[–3]	7.39[–4]	1.41[–3]	2.54[–3]	2.57[–3]	3.75[–3]
4.04		6.42[–4]	7.74[–4]	1.69[–3]	6.76[–4]	9.05[–4]	1.86[–3]	1.57[–3]	2.54[–3]

Peak I consists of the excitations to $4p^5 4d[3/2]_1$ and $4p^5 6s[3/2]_1$, which correspond to the electric dipole allowed excitations to $4p^5(4d, 5d, 6s)^1P_1$. Here the sum of the GOSs for the excitations to $4p^5 4d[3/2]_1$ and $4p^5 6s[3/2]_1$ is presented in Fig.4. It can be seen that the GOS curve decreases with the increasing of momentum transfer at lower values of K^2, which is the typical character of the dipole allowed transition. Furthermore, the GOS curve has a minimum ($K^2 = 1.5 \pm 0.2$ a.u.) and a maximum ($K^2 = 2.8 \pm 0.2$ a.u.)

(see the inset). The solid line in Fig.4 is the fitted result using expression (4), and the extrapolated OOS is 0.26, which is in good agreement with the dipole (e, e) result of 0.24.[30] The GOSs for peaks F and I are listed in Table 2.

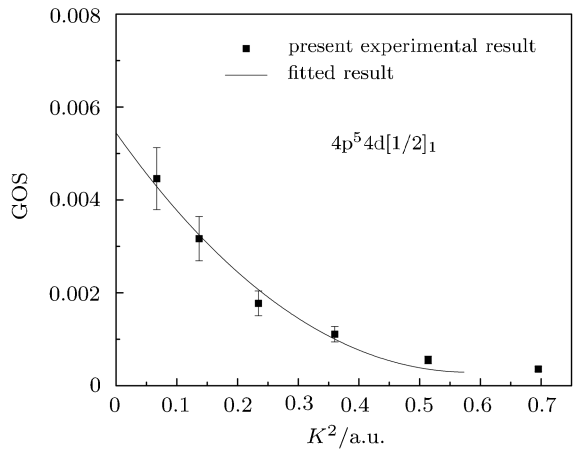


Fig.3. The GOS for the peak F.

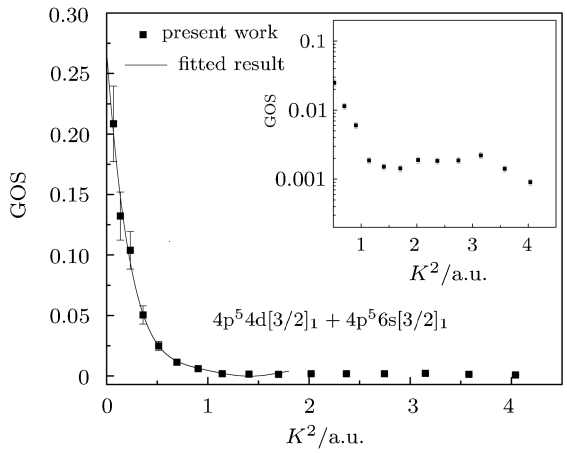


Fig.4. The GOS for the peak I. The extrema at large K^2 region can be seen clearly in the inset.

Secondly, we discuss the GOSs for the dipole forbidden transitions of 5p ← 4p. The GOS for the electric quadrupole excitation in 5p ← 4p was determined with the sum of the GOSs for excitations to $4p^5 5p[5/2]_2$ (peak C) and $4p^5 5p[3/2]_2$ (peak D)[17] divided by the sum of the squares of their intermediate coupling coefficients of the singlet component $4p^5 5p^1D_2$,[6] and it is shown in Fig.5. The result calculated by Amusia *et al*[19] using the method of random phase approximation with exchange (RPAE) is also presented for comparison. It can be seen that the theoretical and experimental GOS profiles are similar, but there is obvious difference for the extremum positions. As for the electric monopole excitations of $4p^5(5p, 5p')[1/2]_0$, although there are the configuration interactions between $4p^5 5p^1S_0$ and $4p^5 6p^1S_0$ according to their intermediate coupling coefficients, the contributions from $4p^5 6p^1S_0$ to GOSs of $4p^5(5p, 5p')[1/2]_0$ can be neglected because the corresponding intermediate coupling coefficients are much lower than those of $4p^5 5p^1S_0$. Therefore, the GOS for the electric monopole excitation in 5p ← 4p was obtained by summing the GOSs for the excitations to $4p^5 5p[1/2]_0$ (peak E)[17] and $4p^5 5p'[1/2]_0$.[6] The result is shown in Fig.6 and compared with the result calculated by Amusia *et al*[19] using the method of RPAE. It can be seen that the theoretical GOS curve has only one maximum while our measured one has two maxima. This indicates that further experimental and theoretical investigations for the electric monopole and electric quadrupole excitations in 5p ← 4p are greatly recommended.

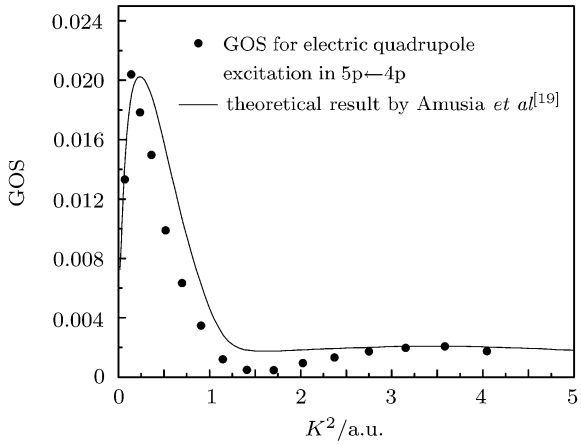


Fig.5. The GOS for the electric quadrupole excitation in 5p ← 4p.

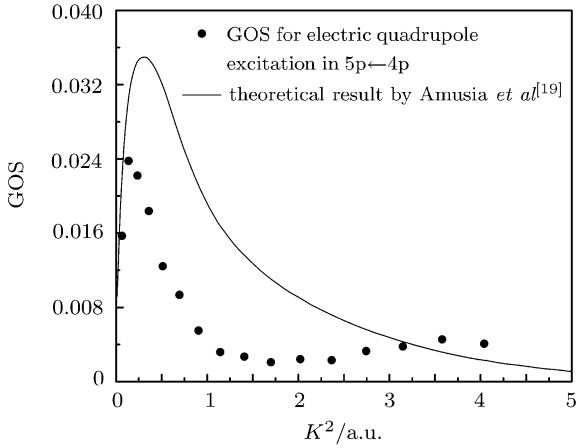


Fig.6. The GOS for the electric monopole excitation in 5p ← 4p.

Thirdly, we discuss the peaks of J, K and L, and each of them contains both dipole-allowed and dipole-forbidden transitions. Since the energy separations

between these high excitations are very small as mentioned above, we can only determine the GOSs for peaks J, K and L, which are listed in Table 2 and presented in Figs.7, 8 and 9, respectively.

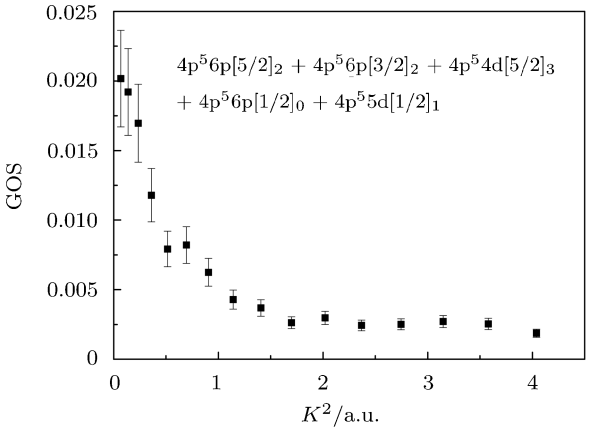


Fig.7. The GOS for the peak J.

Peak J consists of the excitations to $4p^56p[5/2]_2$, $4p^56p[3/2]_2$, $4p^54d[5/2]_3$, $4p^56p[1/2]_0$ and $4p^55d[1/2]_1$, and its GOS is shown in Fig.7. It can be seen from Fig.7 that the GOS values in the lower K^2 region are larger than the OOS 0.0158 of $4p^55d[1/2]_1$.[30] This is because of the contributions from $4p^56p[3/2]_2$, $4p^56p[5/2]_2$, and $4p^56p[1/2]_0$ (here the contribution from the octupole transition of $4p^54d[5/2]_3$ can be neglected due to its very low values[6]). This is also the reason why the GOS curve decreases slowly in the lower K^2 region compared with other dipole transitions (Figs.3 and 4). There is a dip at $K^2 = 0.52$ a.u. which should be due to the joint effect of the five transitions, since the GOS curves for the monopole transition of $4p^56p[1/2]_0$, the quadrupole transitions of $4p^56p[5/2]_2$ and $4p^56p[3/2]_2$, and the dipole transition of $4p^55d[1/2]_1$ decrease rapidly in 0.3 a.u. $< K^2 <$ 1 a.u.,[17,19] while the GOS curve of the octupole transition $4p^54d[5/2]_3$ increases quickly in this K^2 region.[6] Peak K consists of two dipole-allowed transitions to $4p^54d[3/2]_1$ and $4p^56s[1/2]_1$ and two dipole-forbidden octupole-allowed transitions to $4p^55d[7/2]_3$ and $4p^55d[5/2]_3$. It can be seen that the GOS curve presented in Fig.8 decreases with the increasing of momentum transfer at lower values of K^2, it is the typical character of dipole allowed transition. This phenomena can be easily understood since the strengths of the electric octupole excitations are rather weak compared with those of the dipole-allowed transitions, especially for the lower K^2 region.[6] As discussed above, the shoulder at $K^2 = 0.70$ a.u. should be due to the contributions from the electric octupole excitations. The solid line is for the fitted result using expression (3), and extrapolated OOS is 0.052, which is in good agreement with the dipole (e, e) result of 0.0529.[30] Peak L arises from the excitations to $4p^55d[3/2]_1$, $4p^57s[3/2]_1$, $4p^54f[3/2]_2$, $4p^54f[5/2]_2$, and $4p^54f[7/2]_4$.The profile of GOS for Peak L presented in Fig.9 is similar to that for Peak K, the strengths of the two electric dipole-allowed excitations are much stronger than those of the other three excitations. And the extrapolated OOS is 0.18, which is in good agreement with the dipole (e, e) result of 0.1778.[30]

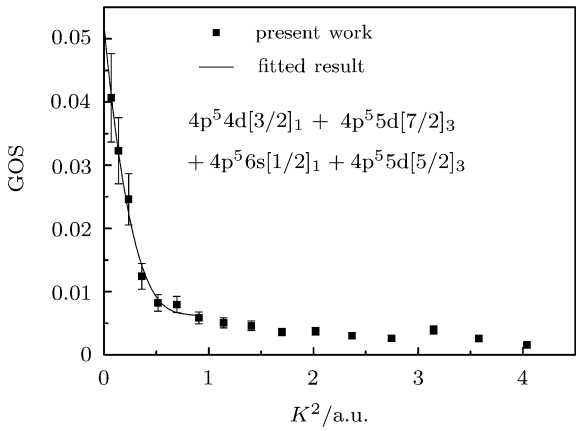


Fig.8. The GOS for the peak K.

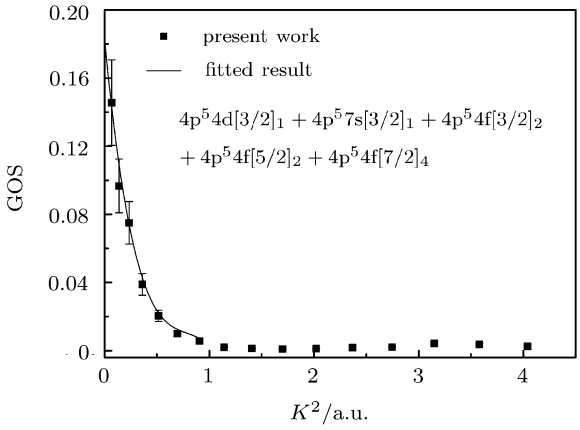


Fig.9. The GOS for the peak L.

4. Conclusion

The GOSs for the valence shell excitations of peaks F–L, which correspond to the excitations to 4d, 4f, 5p, 5d, 6s, 6p, and 7s, have been measured at the incident electron energy of 2500 eV and in the K^2 region of $0.07 - 4.04$ a.u.. To the best of our knowledge, they are reported for the first time. The GOSs

for the electric monopole and the electric quadrupole excitations in 5p ← 4p, as well as the electric dipole in 4d ← 4p, are determined with the help of our calculated intermediate coupling coefficients. Through comparing the present experimental results with the theoretical calculations of Amusia *et al*[19] in the random phase approximation, it is found that the present GOS curves of both the electric monopole and electric quadrupole excitations in 5p ← 4p have two maxima, while the theoretical curve for the electric monopole excitation has only one maximum. Although the theoretical GOS curve for the electric quadrupole excitation in 5p ← 4p has two maxima, there are apparent differences in the extremum positions. Therefore, we expect the present high-resolution work to motivate the further experimental and theoretical investigations. Furthermore, we have noticed that recently Qu and Peng[31] have calculated the Rydberg and autoionization spectra of krypton across the first ionization threshold using their developed relativistic multichannel theory, and we hope that such a theoretical method can be developed to study the problems discussed in this work.

References

[1] Inokuti M 1971 *Rev. Mod. Phys.* **43** 297

[2] Turci C C, Francis J T, Tyliszczak T, Souza G G de and Hitchcock A P 1995 *Phys. Rev.* A **52** 4678

[3] Ge Z M, Zhou Y J, Lu Z W and Wang Z W 2002 *Chin. Phys.* **11** 915

[4] Sun J F, Xu B, Liu Y F and Shi D H 2005 *Chin. Phys.* **14** 1125

[5] Su G L, Ren X G, Zhang S F, Ning C G, Zhou H, Li G Q and Deng J K 2005 *Chin. Phys.* **54** 4108

[6] Cheng H D, Zhu L F, Liu X J, Yuan Z S, Li W B and Xu K Z 2005 *Phys. Rev.* A **71** 032714

[7] Zhu L F, Cheng H D, Yuan Z S, Liu X J, Sun J M and Xu K Z 2006 *Phys. Rev.* A **73** 042703

[8] Liu X J, Zhu L F, Yuan Z S, Li W B, Cheng H D, Huang Y P, Zhong Z P, Xu K Z and Li J M 2003 *Phys. Rev. Lett.* **91** 193203

[9] Wu J H and Yuan J M 2003 *Chin. Phys. Lett.* **20** 841

[10] Chen S H, wang F and Li J M 2004 *Chin. Phys. Lett.* **21** 1251

[11] Avdonina N B, Fursa D, Msezane A Z and Pratt R H 2005 *Phys. Rev.* A **71** 062711

[12] Chen Z F and Msezane A Z 2004 *Phys. Rev.* A **70** 032714

[13] Sun J M, Zhong Z P, Zhu L F, Liu X J, Yuan Z S and Xu K Z 2005 *Chin. Phys.* **14** 1378

[14] Fan L L, Zhong Z P, Zhu L F, Liu X J, Cheng H D, Yuan Z S and Xu K Z 2005 *Chin. Phys.* **14** 2478

[15] Bethe H 1930 *Ann. Phys.* (Leipzig) **5** 325
Bethe H 1930 *Z. Phys.* **76** 293

[16] Tian B G and Li J M 1984 *Acta Phys. Sin.* **33** 1401 (in Chinese)

[17] Li W B, Zhu L F, Liu X J, Yuan Z S, Sun J M, Cheng H D, Zhong Z P and Xu K Z 2003 *Phys. Rev.* A **67** 062708

[18] Suzuki T Y, Suzuki H, Ohtani S, Takayanagi T and Okada K 2007 *Phys. Rev.* A **75** 032705

[19] Amusia M Y, Chernysheva L V, Felfli Z and Msezane A Z 2003 *Phys. Rev.* A **67** 022703

[20] Wu S L, Zhong Z P, Feng R F, Xing S L, Yang B X and Xu K Z 1995 *Phys. Rev.* A **51** 4494

[21] Xu K Z, Feng R F, Wu S L, Ji Q, Zhang X J, Zhong Z P and Zheng Y 1996 *Phys. Rev.* A **53** 3081

[22] Liu X J, Zhu L F, Jiang X M, Yuan Z S, Cai B, Chen X J and Xu K Z 2001 *Rev. Sci. Instrum.* **72** 3357

[23] Moore C E 1971 *Atomic Energy Levels* (U. S. GPO Washington D C) Vol.2

[24] Zhu L F, Zhong Z P, Liu X J, Feng R F, Zhang X J and Xu K Z 1999 *J. Phys.* B **32** 4897

[25] Abdallah J J, Clark R E H and Cowan R D *Los Alamos National Laboratory Manual* No. LA-11436-M 1988 Vol. I (unpublished)

[26] Clark R E H, Abdallah Jr J, Csanak G and Kramer S P 1989 *Phys. Rev.* A **40** 2935

[27] Clark R E H, Csana G k and Abdallah Jr J 1991 *Phys. Rev.* A **44** 2874

[28] Cheng H D, Zhu L F, Yuan Z S, Liu X J, Sun J M, Jiang W C and Xu K Z 2005 *Phys. Rev.* A **72** 012715

[29] Lassettre E N 1965 *J. Chem. Phys.* **43** 4479
Klump K N and Lassettre E N 1978 *J. Chem. Phys.* **68** 886

[30] Yuan Z S, Zhu L F, Liu X J, Zhong Z P, Li W B, Cheng H D and Xu K Z 2002 *Phys. Rev.* A **66** 062701

[31] Qu Y Z and Peng Y L 2005 *Chin. Phys. Lett.* **22** 1884